Methanol Reforming Hot Paper

How to cite: *Angew. Chem. Int. Ed.* **2021**, *60*, 26694–26701
International Edition: doi.org/10.1002/anie.202109979
German Edition: doi.org/10.1002/ange.202109979

A Multi-Layer Device for Light-Triggered Hydrogen Production from Alkaline Methanol

Yiou Wang[+], En-Ping Yao[+], Linzhong Wu, Jochen Feldmann,* and Jacek K. Stolarczyk**

Abstract: *It usually requires high temperature and high pressure to reform methanol with water to hydrogen with high turnover frequency (TOF). Here we show that hydrogen can be produced from alkaline methanol on a light-triggered multi-layer system with a very high hydrogen evolution rate up to ca. 1 μmol s^{-1} under the illumination of a standard Pt-decorated carbon nitride. The system can achieve a remarkable TOF up to 1.8 × 10^6 moles of hydrogen per mole of Pt per hour under mild conditions. The total turnover number (TTN) of 470 000 measured over 38 hours is among the highest reported. The system does not lead to any CO_x emissions, hence it could feed clean hydrogen to fuel cells. In contrast to a slurry system, the proposed multi-layer system avoids particle aggregation and effectively uses light and Pt active sites. The performance is also attributed to the light-triggered reforming of alkaline methanol. This notable performance is a promising step toward practical light-driven hydrogen generation.*

Introduction

Hydrogen is an excellent energy reservoir because of the high gravimetric energy density and clean combustion to water.[1] However, the transport and storage of hydrogen, usually in tanks, remain the difficulty in using hydrogen.[2] In contrast, liquid fuels are more convenient to store and transport and possess relatively high volumetric energy density.[3] Therefore, the in situ generation of hydrogen from inexpensive and stable liquid media offers an attractive alternative and has attracted much attention.[4] The use of water as a proton source to produce hydrogen is known as water splitting, for example, via photolysis or electrolysis under moderate conditions (e.g. 25 °C and 1 atm).[5] While very appealing, this is a challenging reaction both from thermodynamic and kinetic standpoints due to the significant required energy input ($H_2O \rightarrow H_2\uparrow + 1/2\,O_2\uparrow$, $\Delta G = +237\ kJ\,mol^{-1}$) and considerable intermediate energy barriers, respectively. Recent benchmarks in photocatalytic water splitting include the $SrTiO_3$:La,Rh/Au/$BiVO_4$:Mo particulate sheet with a solar-to-hydrogen (STH) efficiency of ca. 1 %[6] and the Rh/$SrTiO_3$:Al catalyst with a quantum efficiency of almost unity at 350–360 nm and a turnover frequency (TOF) of 3600 moles of hydrogen per mole Rh per hour.[7] Compared with photocatalytic water splitting, hydrogen evolution from thermocatalytic aqueous-phase reforming of methanol (APRM, $CH_3OH + H_2O \rightarrow CO_2\uparrow + 3\,H_2$, $\Delta G = +9\ kJ\,mol^{-1}$) is less endergonic and has reached an industrial-grade TOF (1.8×10^4 moles of hydrogen per mole of Pt per hour) on Pt/α-MoC catalyst.[3] Nonetheless, heat-driven APRM usually occurs at 190–350 °C under pressures of 20–50 atm and releases carbon dioxide.[3,4d,8] An ideal hydrogen production process should possess a high TOF under mild conditions with zero carbon emission, a combination that has not yet been reported in the literature.

A light-driven aqueous-phase methanol reforming system, also known as the photocatalytic hydrogen production half-reaction system, has the potential to meet these requirements since it can operate under room temperature and ambient conditions.[9] More importantly, the photocatalytic proton reduction to hydrogen on Pt active sites has been reported to proceed at timescales of 10–900 μs, corresponding to a theoretical TOF of 10^6–10^8 moles of hydrogen per mole of Pt per hour.[10] Although the recent developments have improved the hydrogen evolution rates by a few orders of magnitude in photocatalysis, such remarkable TOF has never been achieved. In photocatalytic H_2 production, water is generally considered the proton source, while methanol is commonly used as a hole scavenger to promote the reduction of protons by electrons (Scheme 1 a). In aqueous methanol reforming systems, alkaline conditions have been commonly used to assist the activation of C–H bond or OH bond.[4d,11] In our previous study, increasing the pH significantly increased the rate of hydrogen production.[12] These reports lead us to investigate one potentially favorable reaction to release hydrogen, the reforming of anhydrous methanol with alkali: $CH_3OH + 2\,NaOH \rightarrow Na_2CO_3\downarrow + 3\,H_2\uparrow$, $\Delta G = -123\ kJ\,mol^{-1}$, $\Delta H = -38.5\ kJ\,mol^{-1}$). The reaction is exothermal (cf. Scheme 1 b). This agrees with earlier detailed investigations of the mechanism of methanol reforming, which showed that only the first step needs to overcome substantial energetic barriers.[13] The subsequent steps need very little or no activation energy.[13] In effect, the energy input, in this case,

[*] Dr. Y. Wang,[+] Dr. E.-P. Yao,[+] L. Wu, Prof. J. Feldmann, Dr. J. K. Stolarczyk
Chair for Photonics and Optoelectronics
Nano-Institute Munich, Department of Physics
Ludwig-Maximilians-Universität München
Königinstrasse 10, 80539 Munich (Germany)
E-mail: yiou.wang@lmu.de
jochen.feldmann@lmu.de
jacek.stolarczyk@physik.uni-muenchen.de

[+] These authors contributed equally to this work.

Supporting information and the ORCID identification number(s) for the author(s) of this article can be found under: https://doi.org/10.1002/anie.202109979.

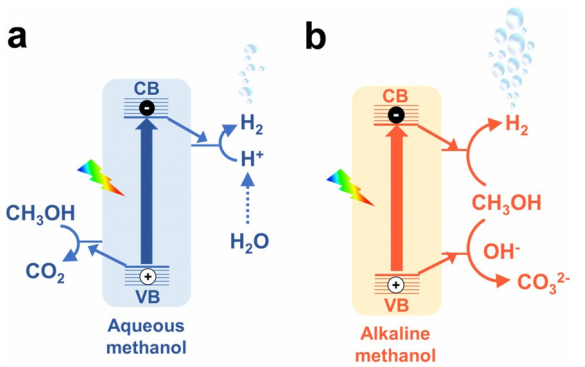

Scheme 1. Photocatalytic hydrogen production from a) aqueous-phase methanol and b) alkaline methanol.

the incident light, is only required to trigger the first step while the following reactions can proceed favorably without the need for harsh high-temperature and high-pressure conditions.

A slurry system, where catalysts disperse in a liquid medium, is the most commonly used system in photocatalytic hydrogen production due to its simplicity for evaluating catalytic performance.[12,14] A slurry system is challenging to scale up because it is constrained by the need for extra energy input for agitation to avoid the precipitation of the catalysts. The particle aggregation, non-uniform distribution of the catalyst and light-scattering losses also need to be dealt with for potential large-scale use.[15] Therefore, a non-slurry design might offer a more practical approach with controllable management of light and catalysts as well as a high TOF on active sites.

Herein, we report that hydrogen could be released from alkaline methanol in a multi-layer system with TOF up to 1.8×10^6 moles of hydrogen per hour per mole of Pt (0.01% Pt-decorated carbon nitride, Pt/CN) or with a hydrogen evolution rate up to ca. 1 $\mu mol\,s^{-1}$ (1% Pt/CN) under light illumination. Such a TOF is two orders of magnitude higher than that in thermal catalytic APRM. It can also reach a high total turnover number (TTN) of 470000, which is among the highest reported. We attribute this unprecedented activity to the light-triggered anhydrous alkaline methanol reaction and the multi-layer architecture of the transparent membrane coated with photocatalysts, which avoids particle aggregation, allows for tuning of the light propagation and works without the need for agitation. Moreover, there is no carbon emission to the gas phase as CO_2 is captured in carbonate.

Results and Discussion

The idea of the present study is to immobilize the photocatalyst particles on the transparent polypropylene (PP) substrate for the reaction of methanol reforming to hydrogen under light (Figure 1a). Such a PP substrate could be folded into multi-layer structures to harvest the incident photons over the whole sample (Figure 1b). In this study, we focused on the hydrogen generation process instead of trying out new materials. We hence chose two well-documented materials, CN and TiO_2, as photocatalysts and commonly used

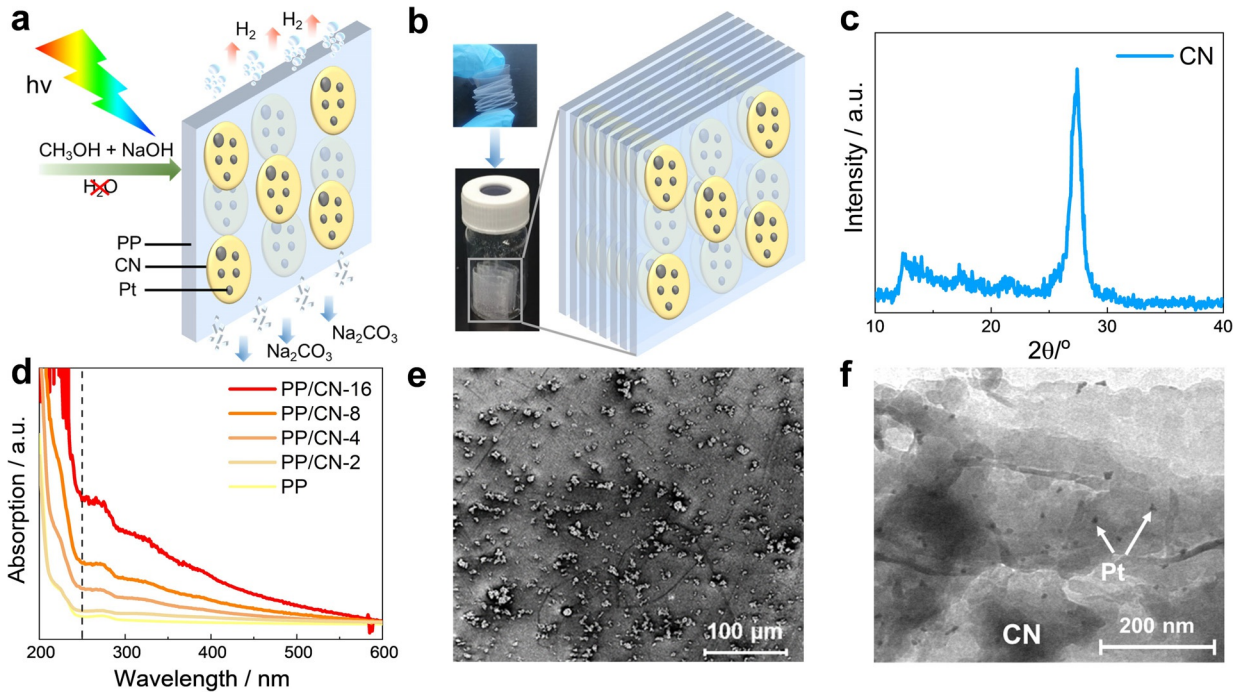

Figure 1. Fabrication and characterizations of the multi-layer system. a) The single PP layer decorated with Pt/CN for alkaline methanol reforming to hydrogen under light. b) The multi-layer membrane for alkaline methanol reforming to hydrogen. Inset: images of a bendable multi-layer membrane before and after deposition of Pt/CN. c) PXRD pattern of CN. d) UV/Vis spectra of PP and the Pt/CN-decorated PP membranes in this study. PP–*x*, where *x* stands for the numbers of coated layers. e) SEM image of CN on PP membrane. f) TEM image of Pt on CN. The loading of Pt on CN in a sample shown is 3% w.t.

Pt as the co-catalyst. The CN photocatalyst was synthesized from urea, while TiO_2 was commercial P25 used without further treatment.[1,16] Powder X-ray diffraction (PXRD) (Figure 1c) was first used to determine the crystal structure of the prepared CN. Two peaks locating at 12.5° and 27.4° were observed, which are assigned to the (100) and (002) planes, respectively, corresponding to intralayer packing size of 7.07 Å and an interlayer distance of 3.26 Å.[16a] Other experimental details can be found in the Supporting Information (SI).

Briefly, a sheet of PP was folded into a multi-layer consisting of 32 2×2 cm^2 single layers. This multi-layer substrate was cleaned with water and 2-propanol and dried before being placed in an oxygen plasma cleaner to increase the hydrophilicity of the surface (Figure S1). Then, for example, 2 mg of Pt/CN were loaded on both sides of the PP substrate and dried in an oven at 70 °C before placing it in a 30 mL gas-tight reactor (Figure S1). The distribution of catalysts and, thereby, the light absorption have been carefully tailored by varying the loading of the catalyst on the film and the number of layers (Figure 1d). To check the reproducibility, we calculated the average weight difference before and after loading as the mass of coated CN (Table S1) for a series of 8 samples. The standard deviation was only about 5% (1.04 ± 0.05 mg CN per 16-layer), meaning the loading does not introduce much uncertainty. PP hardly absorbs sunlight (Figure 1d and S2), ensuring that light is absorbed only by the catalysts. From scanning electron microscopy (SEM) (Figure 1e and Figure S3a,b), CN clusters with a size of below ca. 2 μm could be discerned on the PP substrate. The semiconductor photocatalysts, CN and TiO_2, were decorated with Pt via photodeposition,[16a] forming Pt/CN and Pt/TiO_2 samples, respectively. As shown in Figure S4, no CN particles were observed on the blank substrate, excluding that the observed particles in Figure 1e were an impurity. EDS mapping of the CN-coated sample shows the uniform presence of carbon, as expected, because the substrate is polypropylene. CN coating is indicated by the detection of nitrogen in some regions of the substrate. The transmission electron microscopy (TEM) images (Figure 1f and Figure S3c) of Pt/CN show a stacked-layer morphology of CN and Pt clusters with a size of around 2–5 nm. The obtained Pt/CN coating on PP remains robust even after rinsing with water and methanol.

The proposed reaction contains only sodium hydroxide, methanol and a negligible amount of water. According to our previous findings, such strong alkaline conditions were reported to prolong the lifetime of photogenerated electrons by quickly eliminating the photoholes by OH^- to form hydroxyl radicals, which react with alcohol at a high rate.[12] The slow hole transfer process is then replaced with two faster ones, leaving long-lived electrons to reduce protons to hydrogen efficiently.[12] The presence of a high concentration of OH^- also aids the deprotonation of methanol and potentially captures the CO_2 into carbonates, which could be later determined by the XRD of the product (Figure S5a).[12,17] The photocatalytic experiments were then carried out on the multi-layer system in a 10 mL NaOH solution in methanol under light irradiation.

Both the TOF and real hydrogen formation rate are important to evaluate the performance of a catalyst, hence both are discussed. The hydrogen evolution rates are presented in both commonly used units of "$\mu mol\,s^{-1}$" and "$\mu mol\,gs^{-1}$" (Table S2) to describe the activity clearly. In addition, to exclude reproducibility issues, at least three repeated experiments were carried out for each point. Error bars are shown in all Figures. First, we measured the hydrogen production rates on 3% w.t. Pt/CN multi-layer samples in four NaOH methanol solutions containing 3%, 2%, 1% and 0% (v/v) water, respectively, to investigate the influence of water content (Figure 2a). As the water amount decreased, both hydrogen production rates and TOF increased. In the absence of water, the sample evolved hydrogen at a rate of 241.7 $\mu mol\,gs^{-1}$ or 0.48 $\mu mol\,s^{-1}$ with an average TOF of 6×10^3 moles of hydrogen per mole of Pt per hour, generating visible bubbles during the catalytic process (Figure 2a and the Supporting Video). Water is a widely used proton source. However, extra water here appears detrimental to photocatalytic hydrogen production from alkaline methanol, where methanol acts as both the proton source and the hole scavenger, likely because it is more challenging to deprotonate methanol in the presence of water. The system is anhydrous at the beginning, which already ensures a noticeable enhancement in the activity. However, water could be produced in situ by oxidation or deprotonation of methanol under highly alkaline conditions,[12,17b,18] enabling a side reaction of aqueous methanol reforming. It is important to note that aqueous methanol reforming is endothermal while the reforming of alkaline methanol is exothermal. The system with extra water is thermodynamically more challenging. Such a reaction would likely decrease the overall performance of hydrogen production on a longer timescale (see discussions below).

In contrast to the multi-layer system, the conventional slurry system used as a reference showed 30-fold lower hydrogen production rate and TOF (Figure 2b). Such a dramatic difference indicates that the well-distributed photocatalyst on the multi-layer system can utilize the incident photons much more efficiently than a slurry system under identical conditions. To exclude that the PP substrate might react with the Pt/CN, we sliced a piece of PP substrate (32-fold 2×2 cm^2, pre-treated under identical conditions) and added it into a reference Pt/CN stirred slurry (Figure 2b). No significant improvement in the hydrogen production rate was observed, indicating the stability of the PP substrate. In the slurry system, the anhydrous alkaline methanol system also showed 20 times higher activity than a typical aqueous photocatalytic system containing 10% methanol (Table S2, Entry 5 and 6).

To confirm the hypothesis of improved light harvesting by the multi-layer device compared to a slurry, the UV/Vis absorption measurements were carried out in both systems containing CN of an identical concentration. It could be observed that the major absorption of CN (around 400 nm) on a multi-layer device is much stronger (ca. 4 times higher intensity) than the slurry system (Figure 2c). On the other hand, we also used dynamic light scattering (DLS) to detect the average diameters of CN particles in a slurry and on

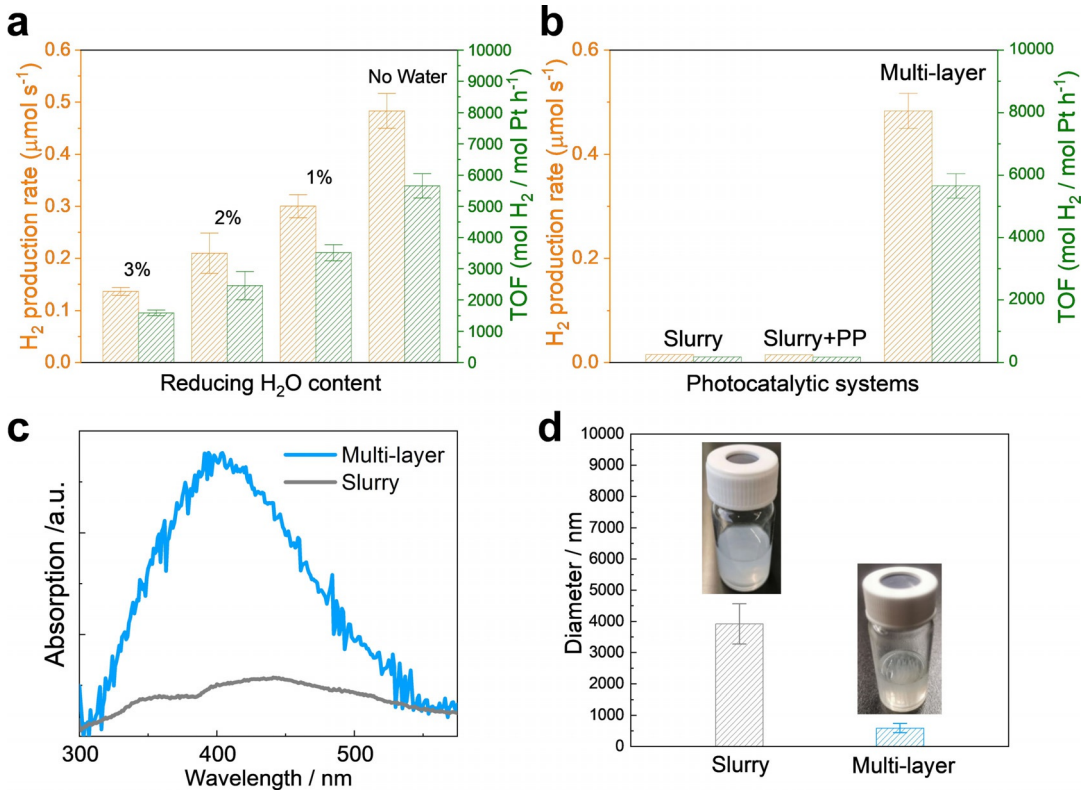

Figure 2. a) Hydrogen production rates and TOFs as a function of the amount of water in the multi-layer system from alkaline methanol reforming. b) Hydrogen production rates and TOFs of the multi-layer system (32-fold), the slurry system and the slurry with PP flakes. c) UV/Vis absorption spectra of CN on a multi-layer structure and in a slurry system with an identical concentration. Concentration: 1 mg/10 mL. d) The comparison of the average diameter of CN between a multi-layer structure and a slurry system via DLS measurement with inset images.

a multi-layer device. The average diameter of CN in a slurry is 3920 ± 640 nm, while that on a multi-layer device is 590 ± 150 nm. Although the size of CN particles varies a lot, the range of a slurry is over six times higher, confirming that the aggregation of particles has been mitigated to some extent by the multi-layer structure (Figure 2d). After the reaction, slightly fewer coated particles could be observed on the substrate, probably due to the peeling off of the coated CN during the reaction (Figure S4c). However, as shown in SEM, the particle size was still mostly below 2 μm, confirming the benefit of prevention of particle aggregation.

In the absence of Pt decoration, a membrane with 2 mg CN produced only a tiny amount of hydrogen (2.8 $\mu mol\,g_s^{-1}$ or 0.01 $\mu mol\,s^{-1}$, Figure S5b), while Pt/CN produces 241.7 $\mu mol\,g_s^{-1}$ (0.48 $\mu mol\,s^{-1}$), that is, almost two orders of magnitude more (Table S2, Entry 8 and 9). Therefore, the hydrogen production proceeds at Pt active sites, while the contribution of pristine CN is negligible. This confirms that the calculation of TOF based on the amount of Pt, considered the provider of the active sites, is reasonable. In further control experiments (Figure S5b and Table S2), negligible hydrogen was detected without light, catalysts or methanol, indicating that such an exothermal reaction is not spontaneous but needs to be triggered by the incident photons. Illumination can naturally raise the temperature of a reactor to 60–70 °C.[9,19] Another possible reason for the temperature rise is the exothermic methanol reforming with alkali. Thus, the temperature of the present system could reach up to 60–70 °C. However, no catalytic activity was observed when the reactor was held at 70 °C under dark conditions (Figure S5b), confirming that light is a necessary factor.

Concerning light management, the geometry of the setup is expected to decrease the number of photons scattered out of the reactor in comparison to the vial with a slurry. To manage the light propagation inside the system, we tuned the numbers of stacking layers from 32 to 16 to 8 (2.0, 1.0 and 0.5 mg of Pt/CN, respectively). The optimal hydrogen production was achieved on a 16-fold membrane (Figure S6a,b), and the TOF was further increased to 4.4×10^4 mole of hydrogen per mole of Pt per hour with a hydrogen formation rate of 189 $\mu mol\,g_s^{-1}$ or 0.19 $\mu mol\,s^{-1}$.

Platinum is typically seen as the cost determinant of a methanol reforming system. Excess Pt shields the surface of CN from incident photons and decreases the number of individual sites by forming large clusters. Therefore, it is crucial to use these active sites adequately to maximize the TOF. One method is to load Pt-decorated CN powder on the PP. In this case, some Pt sites were presumably embedded inside the CN (Figure 3a, left), out of the reach of the protons at the methanol/CN interface and thus wasted for activity. Consequently, CN was first coated on the membrane to decorate Pt exclusively on the surface of CN. Pt was in situ photodeposited on CN (Figure 3a right). With an identical amount of Pt (0.3 % w.t. CN), the in situ Pt-loaded sample

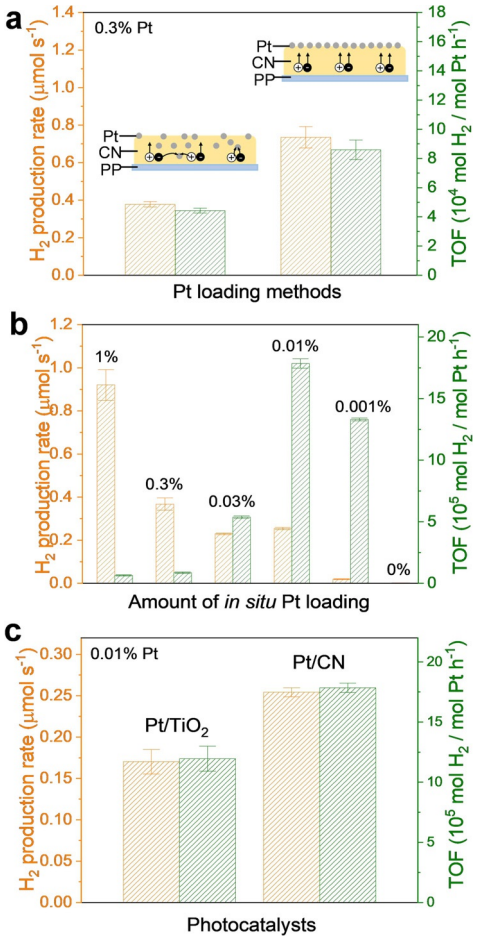

Figure 3. a) Hydrogen production rates and TOFs as a function of the Pt loading methods from alkaline methanol reforming. Left: typical loading method, Pt dispersed randomly in CN. Right: in situ loading method, Pt selectively loaded on the interface of methanol/CN. b) Hydrogen production rates and TOFs as a function of the amount of Pt in situ loaded on CN. c) Hydrogen production rates and TOFs as a function of different photocatalysts (TiO_2 and CN) in situ coated with Pt co-catalyst.

exhibited a higher activity compared with the sample with CN pre-decorated with Pt (Figure 3a).

As the loading ratio changed from 1% to 0.3%, the TOF increased by 13% (Figure 3b). Approximately 1 $\mu mol\,s^{-1}$ (0.9 $\mu mol\,s^{-1}$ or 920 $\mu mol\,gs^{-1}$) activity was achieved on a 1% Pt/CN sample, as shown in Figure 2b and Table S2, Entry 17, corresponding to a TOF of ca. 6×10^4. Reducing the amount of Pt to 0.03% w.t. of CN, the TOF reached 5×10^5 mole of hydrogen per mole of Pt per hour. Interestingly, the 0.01% Pt/CN sample produced hydrogen with a TOF reaching 1.8×10^6 mole of hydrogen per mole of Pt per hour with an internal quantum yield of 21% at 365 nm and a hydrogen evolution rate of 254 $\mu mol\,gs^{-1}$ or 0.25 $\mu mol\,s^{-1}$. The hydrogen evolution rate of 254 $\mu mol\,gs^{-1}$ is the third-highest among all the samples, even higher than the 3% Pt/CN (typical Pt loading, Table S2, Entry 9). The sample thus combines the highest TOF, the third-highest hydrogen evolution rate and the lowest noble metal loading amount, hence it has been chosen as the representative sample in our study. We have also measured the activity of 0.001% Pt/CN. The average TOF reaches 1.3×10^6, that is, slightly smaller than the 0.01% Pt/CN. Accordingly, the H_2 evolution rate (not normalized by the mass of Pt) dropped to 0.02 $\mu mol\,s^{-1}$. This activity is much less than that of 0.01% Pt/CN (0.25 $\mu mol\,s^{-1}$), in fact quite close to that of pristine CN (0.01 $\mu mol\,s^{-1}$). Such a drop indicates that without a sufficient number of active sites, hydrogen could not be produced at a high rate. We emphasize that the observed dramatic enhancement here is also attributed to the selective deposition of exposed Pt active sites on the surface of photocatalysts, besides the use of anhydrous alkaline methanol and multi-layer structure.

We have carried out the ICP-OES measurements to quantify the exact Pt amount in 0.01% Pt/CN samples loaded via both the in situ and typical photodeposition method. 100 ng of Pt was added in each run to obtain the 1 mg 0.01% w.t. Pt/CN catalyst. The measured actual Pt amounts are 82.9 ± 1.2 ng for the in situ photodeposition and 43.2 ± 0.1 ng for the typical method. This implies that the TOFs based on used Pt amount were in fact underestimated. Interestingly, the amount of actual loaded Pt by the in situ method was double that obtained by the typical method which potentially explains the higher H_2 production achieved with the former method.

To investigate the compatibility of our system with different photocatalysts, we loaded P25 TiO_2 nanoparticles onto a multi-layer PP substrate using identical methods (Figure S6c). A reproducible hydrogen production rate of 170.2 $\mu mol\,gs^{-1}$ or 0.17 $\mu mol\,s^{-1}$ was measured on Pt/TiO_2 (Figure 3c and Figure S6d), corresponding to a TOF of 1.2×10^6 mole of hydrogen per mole of Pt per hour. The comparable performance observed on Pt/TiO_2 and Pt/CN indicates that the key for the remarkable activity is the intrinsic beneficial multi-layer structure photocatalytic system and the anhydrous alkaline methanol reforming reaction. This implies that the proposed approach is a general method to speed up the hydrogen production from methanol, and it does not depend on specific semiconductors. The hydrophilicity of semiconductors also influences photocatalytic activities in aqueous systems.[20] In this methanol-based system, other semiconductors with low hydrophilicity might also be used for hydrogen production.

Moreover, the long-term stability of such a multi-layer system loaded with Pt/CN was evaluated. In a 30 mL reactor, the rapid production of hydrogen markedly increases the pressure (ca. 23.2 mL H_2 produced per hour on 1 mg 0.01% w.t. Pt/CN) when the long-term test was carried out under full light power of 450 W. Therefore, to minimize the change in pressure, we decreased the light intensity and placed the reactor inside a bigger sealed container to alleviate the problems with overpressure. This system (Figure 4a and Figure S7d) maintained stable activity over 38 hours with a TOF equal of 1.6×10^4 and a total turnover number of 470000. The TOF is comparable to the benchmark of hydrogen production from methanol reforming, that is, from a thermal catalytic system (stability of 10 hours with TOF of 1.8×10^4),[3] and the TON is among the highest reported (cf. Table S3). To understand whether the photocatalyst is stable

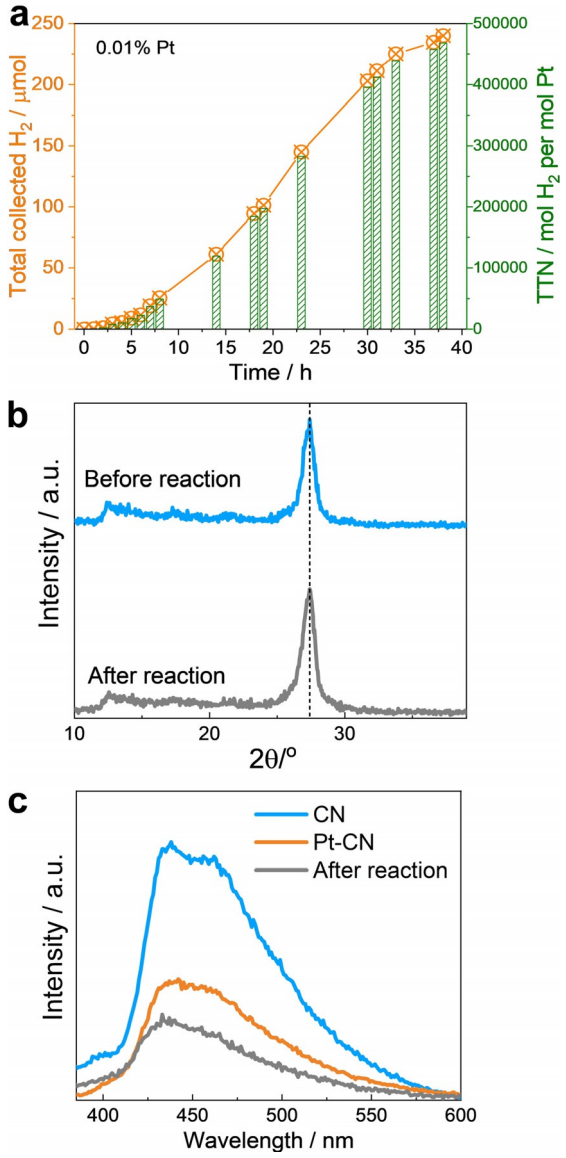

Figure 4. a) Approaching long-term alkaline methanol reforming on 0.01 % Pt/CN under weak light conditions for 38 hours. TTN: total turnover number. b) PXRD and c) PL spectra of CN and Pt/CN before and after reaction.

during the reaction, we carried out the PXRD and PL measurements before and after the long-term reaction. As shown in Figure 4 b, no noticeable difference was observed on the characteristic PXRD pattern, indicating that the CN was unchanged. According to the PL spectra (Figure 4 c, excitation at 325 nm), it is observed that the signals were quenched after the loading of Pt on CN. The PL spectra of samples after the reaction stay at a low intensity, similar to those Pt/CN before reaction rather than the pristine CN. This clearly indicates that the function of Pt is stable after the long-term reaction.

During the oxidation of methanol, there is potentially water produced during the reaction.[13] Therefore, the side reaction of aqueous methanol reforming may occur in the system. However, as shown in Figure 2, the hydrogen production performance without water is superior to the one with water. Such a side reaction of aqueous methanol reforming would likely decrease the overall performance of hydrogen production in the long term. Distinguishing the effect of water amount and pH of the solution is challenging because both factors are interdependent. In previous work, pH significantly influenced the activity below pH of 15.[12] Moreover, in 97–100 % methanol, it would be difficult to determine the pH since the activities would be different from that in a dilute aqueous solution. Nonetheless, it will be worth further study to investigate the effect of the concentration of hydroxyl anions and water molecules on the reaction mechanism.

We have confirmed the product of Na_2CO_3 from the reaction by XRD (Figure S5a). The major signals are assigned to Na_2CO_3, confirming the proposed pathway of the reaction together with the gas phase detection of hydrogen as the main product. We have separated the produced insoluble Na_2CO_3 from methanol. As calculated, the average ratio between H_2 (881.4 µmol) and Na_2CO_3 (424.5 µmol) for three runs is around 2.1, indicating that the proposed overall reaction equation is reasonable. A smaller ratio below the ideal 3:1 ratio is likely due to leakage and underestimation of hydrogen during the measurement due to its overpressure in the reaction vessel. The slight decline of TOF over 38 hours is also partially owing to the reduced transparency of the solution due to the generated Na_2CO_3,[21] which is poorly soluble in methanol (Figure S7). The limited solubility of Na_2CO_3 might also be an advantage because it leads to its separation from the reaction medium. First, it can be collected by capturing the carbon from methanol. Second, the removal of one of the products pushes the reaction equilibrium towards the products, according to the Le Chatelier principle. The carbon is thus captured and separated from the system.

Therefore, another additional advantage of the present system is the in situ collection of CO_2. We compared the GC measurements of the headspace of the reactor before and after the reaction, as displayed in Figure S8. No other products have been detected in the gas phase other than H_2. This implies that the reaction indeed proceeded towards the two discussed products. Negligible CO_x (CO_2 or CO) was detected in the gas phase during the reaction (Figure S8), indicating that CO_2 was captured into carbonate rather than directly released into the headspace. More importantly, the danger of the presence of CO is mitigated. Hence, CO, a well-known poison for the Pt catalysts,[22] is absent in this system, allowing for a clean feed of pure hydrogen for, for example, fuel cells. In particular, methanol could be produced via the reduction of CO_2[23] and the oxidation of methane,[24] while NaOH could be regenerated from Na_2CO_3 (see SI), potentially making the proposed system sustainable.[25]

More strikingly, the multi-layer structure also works to reform gas-phase methanol to hydrogen (Figure 5). Instead of using a 10 mL methanol solution, we placed a vial containing 1.5 mL methanol to generate its vapor inside the reactor. NaOH was loaded together with Pt/CN on PP (16-layer 0.01 % w.t. Pt/CN), providing a local alkaline environment (Figure 5 a). Although the amount of reactants compared to the liquid-phase system was significantly reduced, this gas-

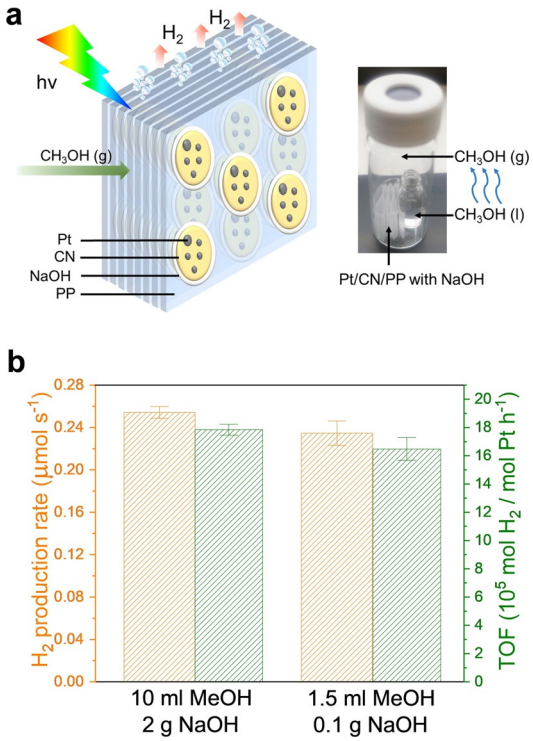

Figure 5. Gas-phase methanol reforming on the multi-layer systems. a) Left: schematic of the multi-layer membrane for gas-phase methanol reforming to hydrogen under light. Right: an image of the methanol vapor reforming setup on multi-layer membrane coated with Pt/CN/NaOH. b) Hydrogen production rates and TOF comparison with different amounts of reactants added in both methanol reforming systems.

phase configuration still provides a comparable rate of hydrogen production (Figure 5b). This implies a more efficient utilization of reactants than the liquid-phase one. The enhanced activity is attributed to the better contact between the catalyst particles and the methanol vapor. This gas-phase methanol reforming system with a high TOF and HER could be further improved for practical application, for example, in a flow system. We also compared the stability of both systems by purging the reactor at a regular interval between each run under normal light intensity. As shown in Figure S9, the hydrogen production rates in methanol liquid start to drop during the five runs and stabilize at a lower rate. This is likely due to the peeling-off issue of the Pt/CN particles from the PP during the reaction. However, the hydrogen evolution rates in the methanol vapor show a stable production for five runs, suggesting the peeling-off effect of catalyst particles can be mitigated in the methanol vapor system.

For the simplicity and to focus on the major aspects of the multi-layer system, in this study, we used a batch closed reactor as a demonstration device exhibiting good stability despite its limitations. However, in a batch reactor setup, the build-up of water from methanol oxidation is found detrimental to the activity, and the issues of the accumulation and separation of Na_2CO_3 during the reaction could not be solved. Future developments, which would likely involve a flow reactor instead of a sealed batch reactor, would eliminate the problems manifesting here. In a potential flow device in the future, Na_2CO_3 could be recycled, and NaOH could also be constantly supplied. This would eliminate the possibility of decreasing activity due to the transparency issue and the depletion of NaOH. In addition, the multi-layer system offers a possibility to tailor the absorption of light by tuning the amount of deposited catalysts on each layer. Such fine-tuning is not possible with a slurry stirred to form a uniform medium. In this context, we believe that a tunable system with 30 times higher activity than a standard slurry system that operates under mild temperature and pressure conditions is potentially opening new design pathways for the methanol reforming systems. To investigate the leaching of the catalyst, we have measured the hydrogen production activity of the device after the storage in alkaline methanol solution after 0, 3, 24 and 72 hours in dark conditions (Figure S10). The activity dropped to half of the original activity, likely due to the peeling-off of Pt/CN particles from the PP. A better coating technique in the future would significantly enhance the stability of the catalyst on the substrate.

Conclusion

In summary, we have shown an efficient process to produce hydrogen from alkaline methanol on a multi-layer device. We demonstrated that the reaction reaches a hydrogen evolution rate up to ca. 1 μmol s^{-1} (1 % Pt/CN) and a TOF up to 1.8×10^6 mole of hydrogen per mole of Pt per hour (0.01 % Pt/CN) on multi-layer architecture loaded with standard photocatalysts Pt/CN or Pt/TiO_2 under light illumination. The proposed layered system shows superior performance compared to the commonly used slurry systems without the need for agitation. The optimal TOF is two orders of magnitude better than reported for the thermal catalytic approach, and the TTN of 470000 measured over 38 hours is among the highest reported. Herein, anhydrous methanol and alkali function as both the proton source and the hole scavenger, where light has a kinetic role as a trigger for the reaction. We consider that the high hydrogen production rate comes from the intrinsically thermodynamically favorable reaction, the prevention of particle aggregation, the light management and the efficient utilization of Pt active sites. Moreover, the system could sustainably reform both the liquid and the gas phase of methanol to feed pure hydrogen to, for example, fuel cells. Furthermore, the earth abundance of raw materials used for the polymer and urea, the inkjet printing technique to deposit catalysts on the membrane and the compatibility of the gas-phase device with a flow system could enable scalable fabrication and hold promise for broad and practical applications.

Acknowledgements

This research work was supported by the Bavarian State Ministry of Science, Research, and Arts through the grant "Solar Technologies go Hybrid (SolTech)" and by the European Union's Framework Programme for Research and

Innovation Horizon 2020 (2014–2020) under the Marie Skłodowska-Curie Grant Agreement No. 754388 (E.-P. Yao) and from LMU Munich's Institutional Strategy LMU excellent within the framework of the German Excellence Initiative (No. ZUK22). Y. Wang thanks the Alexander von Humboldt Foundation for a fellowship. L. Wu thanks the China Scholarship Council (CSC). We thank local research clusters and centers such as the Center of Nanoscience (CeNS) and e-conversion for providing communicative networking structures. We also thank Dr. He Huang, Nathalie Schmid, Jianian Chen and Sophie Gutenthaler for their assistance on TEM, SEM-EDS, ICP-OES measurements and video filming. Open Access funding enabled and organized by Projekt DEAL.

Conflict of Interest

The authors declare no conflict of interest.

Keywords: alkaline · methanol reforming · multi-layer structure · photocatalytic hydrogen production · TOF

[1] Y. Wang, A. Vogel, M. Sachs, R. S. Sprick, L. Wilbraham, S. J. A. Moniz, R. Godin, M. A. Zwijnenburg, J. R. Durrant, A. I. Cooper, J. Tang, *Nat. Energy* **2019**, *4*, 746 – 760.

[2] L. Schlapbach, A. Züttel, *Nature* **2001**, *414*, 353 – 358.

[3] L. Lin, W. Zhou, R. Gao, S. Yao, X. Zhang, W. Xu, S. Zheng, Z. Jiang, Q. Yu, Y.-W. Li, C. Shi, X.-D. Wen, D. Ma, *Nature* **2017**, *544*, 80.

[4] a) B. C. H. Steele, A. Heinzel, *Nature* **2001**, *414*, 345 – 352; b) J. A. Turner, *Science* **2004**, *305*, 972 – 974; c) J. K. Norskov, C. H. Christensen, *Science* **2006**, *312*, 1322 – 1323; d) M. Nielsen, E. Alberico, W. Baumann, H.-J. Drexler, H. Junge, S. Gladiali, M. Beller, *Nature* **2013**, *495*, 85.

[5] a) R. S. Sherbo, R. S. Delima, V. A. Chiykowski, B. P. MacLeod, C. P. Berlinguette, *Nat. Catal.* **2018**, *1*, 501 – 507; b) L. Lin, Z. Lin, J. Zhang, X. Cai, W. Lin, Z. Yu, X. Wang, *Nat. Catal.* **2020**, *3*, 649 – 655.

[6] Q. Wang, T. Hisatomi, Q. Jia, H. Tokudome, M. Zhong, C. Wang, Z. Pan, T. Takata, M. Nakabayashi, N. Shibata, Y. Li, I. D. Sharp, A. Kudo, T. Yamada, K. Domen, *Nat. Mater.* **2016**, *15*, 611.

[7] T. Takata, J. Jiang, Y. Sakata, M. Nakabayashi, N. Shibata, V. Nandal, K. Seki, T. Hisatomi, K. Domen, *Nature* **2020**, *581*, 411 – 414.

[8] K. M. K. Yu, W. Tong, A. West, K. Cheung, T. Li, G. Smith, Y. Guo, S. C. E. Tsang, *Nat. Commun.* **2012**, *3*, 1230.

[9] J. Zhao, R. Shi, Z. Li, C. Zhou, T. Zhang, *Nano Select* **2020**, *1*, 12 – 29.

[10] A. Yamakata, T.-a. Ishibashi, H. Onishi, *J. Phys. Chem. B* **2001**, *105*, 7258 – 7262.

[11] a) K.-i. Fujita, R. Kawahara, T. Aikawa, R. Yamaguchi, *Angew. Chem. Int. Ed.* **2015**, *54*, 9057 – 9060; *Angew. Chem.* **2015**, *127*, 9185 – 9188; b) E. Hao Yu, K. Scott, R. W. Reeve, *J. Electroanal. Chem.* **2003**, *547*, 17 – 24; c) M. A. Abdel Rahim, R. M. Abdel Hameed, M. W. Khalil, *J. Power Sources* **2004**, *134*, 160 – 169.

[12] T. Simon, N. Bouchonville, M. J. Berr, A. Vaneski, A. Adrović, D. Volbers, R. Wyrwich, M. Döblinger, A. S. Susha, A. L. Rogach, F. Jäckel, J. K. Stolarczyk, J. Feldmann, *Nat. Mater.* **2014**, *13*, 1013.

[13] a) T. J. Held, F. L. Dryer, *Int. J. Chem. Kinet.* **1998**, *30*, 805 – 830; b) C. K. Westbrook, F. L. Dryer, *Combust. Sci. Technol.* **1979**, *20*, 125 – 140.

[14] a) B. Burger, P. M. Maffettone, V. V. Gusev, C. M. Aitchison, Y. Bai, X. Wang, X. Li, B. M. Alston, B. Li, R. Clowes, N. Rankin, B. Harris, R. S. Sprick, A. I. Cooper, *Nature* **2020**, *583*, 237 – 241; b) V. W.-h. Lau, I. Moudrakovski, T. Botari, S. Weinberger, M. B. Mesch, V. Duppel, J. Senker, V. Blum, B. V. Lotsch, *Nat. Commun.* **2016**, *7*, 12165; c) Q. Xiang, J. Yu, M. Jaroniec, *J. Am. Chem. Soc.* **2012**, *134*, 6575 – 6578.

[15] R. L. Romero, O. M. Alfano, A. E. Cassano, *Ind. Eng. Chem.* **1997**, *36*, 3094 – 3109.

[16] a) D. J. Martin, K. Qiu, S. A. Shevlin, A. D. Handoko, X. Chen, Z. Guo, J. Tang, *Angew. Chem. Int. Ed.* **2014**, *53*, 9240 – 9245; *Angew. Chem.* **2014**, *126*, 9394 – 9399; b) J. Liu, Y. Liu, N. Liu, Y. Han, X. Zhang, H. Huang, Y. Lifshitz, S.-T. Lee, J. Zhong, Z. Kang, *Science* **2015**, *347*, 970 – 974; c) X. Wang, K. Maeda, A. Thomas, K. Takanabe, G. Xin, J. M. Carlsson, K. Domen, M. Antonietti, *Nat. Mater.* **2009**, *8*, 76 – 80.

[17] a) S. Ouyang, H. Tong, N. Umezawa, J. Cao, P. Li, Y. Bi, Y. Zhang, J. Ye, *J. Am. Chem. Soc.* **2012**, *134*, 1974 – 1977; b) F. T. Wagner, G. A. Somorjai, *Nature* **1980**, *285*, 559 – 560.

[18] D. W. Wakerley, M. F. Kuehnel, K. L. Orchard, K. H. Ly, T. E. Rosser, E. Reisner, *Nat. Energy* **2017**, *2*, 17021.

[19] a) Q. Wang, M. Nakabayashi, T. Hisatomi, S. Sun, S. Akiyama, Z. Wang, Z. Pan, X. Xiao, T. Watanabe, T. Yamada, N. Shibata, T. Takata, K. Domen, *Nat. Mater.* **2019**, *18*, 827 – 832; b) S. Fang, Z. Sun, Y. H. Hu, *ACS Catal.* **2019**, *9*, 5047 – 5056.

[20] a) M. Miyauchi, A. Nakajima, T. Watanabe, K. Hashimoto, *Chem. Mater.* **2002**, *14*, 2812 – 2816; b) K. Guan, *Surf. Coat. Technol.* **2005**, *191*, 155 – 160.

[21] T. Kawai, T. Sakata, *Nature* **1980**, *286*, 474 – 476.

[22] J. C. Amphlett, K. A. M. Creber, J. M. Davis, R. F. Mann, B. A. Peppley, D. M. Stokes, *Int. J. Hydrogen Energy* **1994**, *19*, 131 – 137.

[23] a) G. A. Olah, *Angew. Chem. Int. Ed.* **2005**, *44*, 2636 – 2639; *Angew. Chem.* **2005**, *117*, 2692 – 2696; b) J. Graciani, K. Mudiyanselage, F. Xu, A. E. Baber, J. Evans, S. D. Senanayake, D. J. Stacchiola, P. Liu, J. Hrbek, J. F. Sanz, J. A. Rodriguez, *Science* **2014**, *345*, 546 – 550; c) Y. Wang, X. Liu, X. Han, R. Godin, J. Chen, W. Zhou, C. Jiang, J. F. Thompson, K. B. Mustafa, S. A. Shevlin, J. R. Durrant, Z. Guo, J. Tang, *Nat. Commun.* **2020**, *11*, 2531; d) Y. Wang, R. Godin, J. R. Durrant, J. Tang, *Angew. Chem. Int. Ed.* **2021**, *60*, 20811 – 20816; *Angew. Chem.* **2021**, *133*, 20979 – 20984.

[24] a) J. Xie, R. Jin, A. Li, Y. Bi, Q. Ruan, Y. Deng, Y. Zhang, S. Yao, G. Sankar, D. Ma, J. Tang, *Nat. Catal.* **2018**, *1*, 889 – 896; b) V. L. Sushkevich, D. Palagin, M. Ranocchiari, J. A. van Bokhoven, *Science* **2017**, *356*, 523 – 527; c) Z. Liu, E. Huang, I. Orozco, W. Liao, R. M. Palomino, N. Rui, T. Duchoň, S. Nemšák, D. C. Grinter, M. Mahapatra, P. Liu, J. A. Rodriguez, S. D. Senanayake, *Science* **2020**, *368*, 513 – 517.

[25] A. Goeppert, M. Czaun, J.-P. Jones, G. K. Surya Prakash, G. A. Olah, *Chem. Soc. Rev.* **2014**, *43*, 7995 – 8048.

Manuscript received: July 26, 2021
Revised manuscript received: August 29, 2021
Accepted manuscript online: October 13, 2021
Version of record online: November 16, 2021

